Geomech. Geophys. Geo-energ. Geo-resour. (2021)7:60
https://doi.org/10.1007/s40948-021-00222-z

ORIGINAL ARTICLE

Canonical solutions for wave anelasticity in rocks composed of two frames

Wave anelasticity solutions in composite rocks

José M. Carcione · Juan E. Santos · Jing Ba

Received: 25 September 2020 / Accepted: 27 January 2021

Abstract Wave anelasticity of the fast P wave at mesoscopic scales is due to energy dissipation by conversion to slow P diffusive modes at heterogeneities much smaller than the wavelength and much larger than the pore size. We consider frames composed of two minerals and study the dissipation effects based on a generalized White plane-layered model, where the interfaces satisfy mixed boundary conditions, i.e., open, closed and partially-open pores. We consider three models to obtain the effective properties. Model 1 is based on effective mineral properties, Model 2 is a generalization of Biot theory to the case of two solids and one fluid, and Model 3 is based on a generalization of White model to the case of three layers. A particular case is that of closed pores at the interface between the layers, where no flow occurs and, consequently, there is no anelasticity and the stiffness modulus is a real quantity and does not depend on frequency. The type of boundary condition highly affects the location of the relaxation peak, which moves from high to low frequencies for decreasing interface permeability. The first two models predict similar locations of the peaks and strength (reciprocal of the quality factor). The results of Model 3 differ due to different distribution of the solid phases, since the frames are not mixed at the pore scale as in Models 1 and 2, but at a mesoscopic scale. These solutions are useful to test modeling algorithms to compute the effective P-wave modulus in more general cases.

Article highlights

- The frames composed of two minerals are considered to analyze the dissipation effects based on a generalized White plane-layered model.
- The three different models are analyzed to obtain the properties perpendicular to layering.
- The type of boundary condition highly affects the location of the relaxation peak, which moves from high to low frequencies for decreasing interface permeability.

J. M. Carcione · J. E. Santos · J. Ba (✉)
School of Earth Sciences and Engineering, Hohai University, Nanjing, China
e-mail: jingba@188.com

J. M. Carcione
National Institute of Oceanography and Applied Geophysics OGS, Trieste, Italy

J. E. Santos
Laboratorio de Geofísica Numérica, Instituto del Gas y del Petróleo, Facultad de Ingeniería, Universidad de Buenos Aires, Buenos Aires, Argentina

J. E. Santos
Department of Mathematics, Purdue University, West Lafayette, USA

Published online: 27 May 2021

Keywords Multimineral porous media · Rocks · White model · Anelasticity · Partially open boundary condition

1 Introduction

Rocks such as sandstones are rarely composed of a single mineral, because they may contain clay, feldspar, dolomite, etc., in addition to quartz (Deer et al. 2013). Gas-hydrate bearing sediments and permafrost, for instance, are composed of three solids, i.e., quartz, clay and gas hydrate (ice). The distribution of the minerals and the scale of the heterogeneities affect the anelastic properties of the rock. In seismic exploration, these properties, represented by the wave velocity and dissipation factor, are essential to obtain information about the microstructure and fluid content of reservoir rocks (e.g., Pride et al. 2003; Carcione et al. 2018).

Theories that generalize the Biot theory to two solid frames are available to obtain the seismic properties of these media (e.g., Carcione et al. 2003, 2005; Gei and Carcione 2003; Ba et al. 2016, 2017). We propose canonical models based on poroelasticity and thin plane layers to study these properties. These models can be useful as reference solutions to test numerical algorithms that compute the complex stiffness moduli using, for example, finite-element quasi-static experiments (Carcione 2014, Section 4.3). The problem is to find the effective seismic properties, i.e., the dispersion and attenuation related to the P-wave stiffness modulus along the direction perpendicular to layering. The properties parallel to layering and, in general, the five independent stiffness components of the equivalent transversely isotropic medium can be obtained as in Cavallini et al. (2017, Section 3) on the basis of the relaxed and unrelaxed elastic constants.

It is well known that mesoscopic loss (modulus dispersion and attenuation) of the fast P wave is due to a loss of energy by conversion to slow P diffusive modes, when the heterogeneities are much smaller than the wavelength but much larger than the pore size [an alternative name for this mechanism is wave-induced fluid-flow (WIFF) attenuation (Müller et al. 2010)]. In rocks, the presence of several minerals is an additional cause of WIFF besides partial (patchy) saturation and porosity (permeability) variations, which implies heterogeneities in the dry-rock stiffness moduli. We consider media composed of two minerals to study the mesoscopic-loss effects, based on a generalized White plane-layered model, where the interface (contact between those media) is characterized by mixed boundary conditions. These include a hydraulic interface permeability to model open, closed and partially-open pores.

We consider three models. Model 1 is based on effective mineral properties obtained with the Hashin-Shtrikmann bounds (e.g., Mavko et al. 2009) and then application of the White model. A similar model is that of Brown and Korringa (1975), who extended the Gassmann equation to the case of a micro-inhomogeneous frame. While Gassmann's equation contains one elastic constant of the mineral, the extended model contains two such constants. Yet this model is seldom used in geophysical practice, as the second constant is hard to measure or infer independently [see, e.g., a discussion in Zimmerman (1991, Eq. 6.7)].

Model 2 is a generalization of Biot theory to two solids and one fluid, based on two mixed frames (Carcione et al. 2000, 2003, 2005, 2010, Santos et al. 2004). As with Model 1, the White model yields the effective properties to obtain the attenuation, depending on the interface hydraulic permeability. Model 3 is based on a generalization of White model to the case of three dissimilar porous layers (Norris 1993; Cavallini et al. 2017). A particular case is that of closed pores at the interface between the layers. This case of no flow between the layers does not imply anelasticity and the stiffness modulus is the Reuss average of the Gassmann moduli of the single layers as predicted by Backus averaging (the high-frequency limit of White model) (Backus 1962; White et al. 1975; Carcione et al. 2006; Carcione 2014, Section 7.13).

2 Theory

Let us consider a periodic system of two thin planar layers, where each layer, denoted with the index j = 1,2, is a porous medium composed of two solids (i = 1,2) and a fluid (f). The fraction of solid i in layer j is ϕ_{ij} such that

$$\phi_{1j} + \phi_{2j} + \phi_j = 1, \tag{1}$$

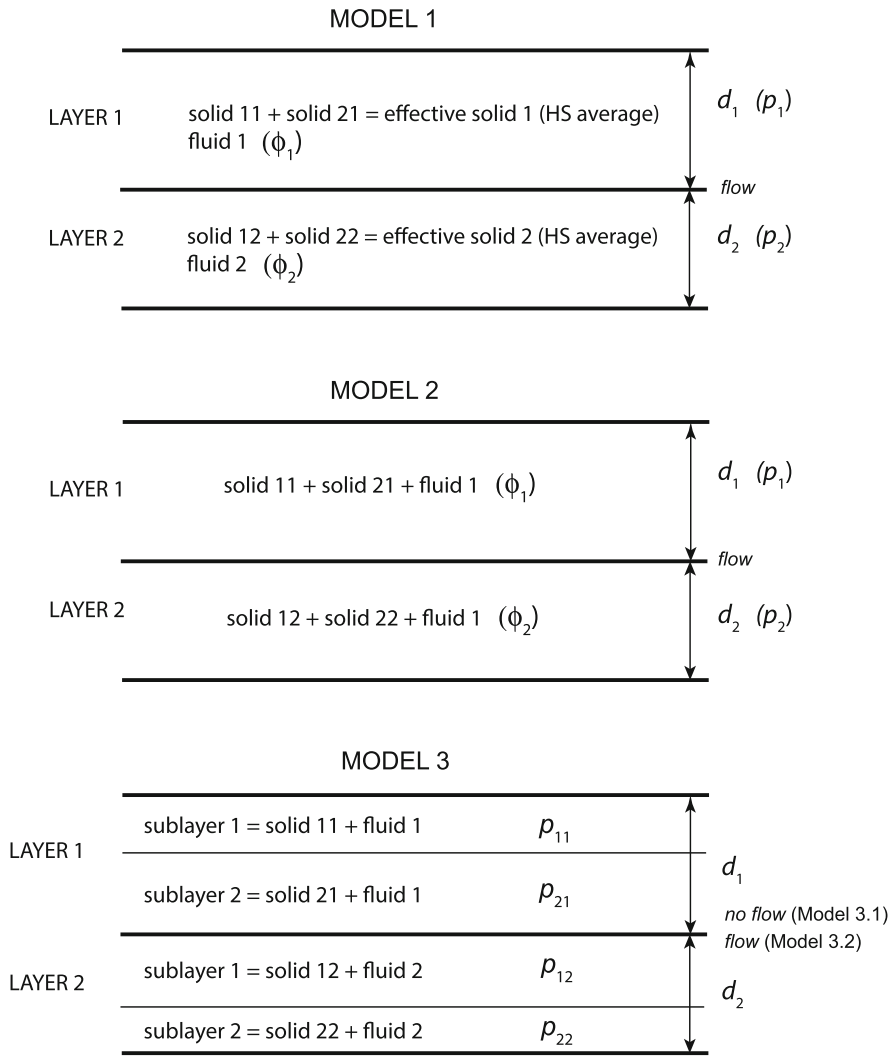

Fig. 1 Three models of mesoscopic attenuation. Flow through layers generates the Biot slow (diffusive) wave, which is responsible of the attenuation of the fast P wave by conversion to slow P wave. Subindices *ij* denote solid *i* in layer *j*.

where ϕ_j is the porosity in layer j. Solid 1 in layer 1 can have different properties compared to solid 1 in layer 2, etc. The thickness of layer j is d_j and the period is $D = d_1 + d_2$, with $p_j = d_j/D$, $j = 1, 2$, being the proportions of each layer. We consider three models as shown in Fig. 1, which yield the P-wave complex modulus, E, in the direction perpendicular to the layering.

2.1 Model 1

Let us omit the layer index j for clarity. A simple approach to obtain the plane-wave modulus normal to the stratification, E, is first to use the Hashin-Shtrikman average to obtain the effective bulk and shear moduli of the solid composing the frame in each single layer, K_s and μ_s (e.g., see Mavko et al. 2009, Fig. 4.17.2). Then, we use the mesoscopic-loss theory of wave propagation through a periodic system of thin plane layers, developed by White et al. (1975), whose basic equations are given in "Appendix 1", where we have introduced an interface permeability as additional property.

Let us denote the solid bulk and shear moduli by K_i and μ_i, respectively. A two-solid composite, with no restriction on the shape of the two phases, has stiffness bounds given by the Hashin and Shtrikman (1963) equations,

$$K_{\mathrm{HS}}^{\pm} = K_1 + \frac{\beta_2}{(K_2 - K_1)^{-1} + \beta_1 \left(K_1 + \frac{4}{3}\mu_\beta \right)^{-1}} \tag{2}$$

and

$$\mu_{\mathrm{HS}}^{\pm} = \mu_1 + \frac{\beta_2}{(\mu_2 - \mu_1)^{-1} + \beta_1 \left[\mu_1 + \frac{\mu_\beta}{6} \left(\frac{9K_\beta + 8\mu_\beta}{K_\beta + 2\mu_\beta} \right) \right]^{-1}}, \tag{3}$$

where β_1 and β_2 are the fractions of solid 1 and 2 ($\beta_1 + \beta_2 = 1$), with $\beta_1 = \phi_1/(1-\phi)$. We obtain the upper bounds when K_β and μ_β are the maximum bulk and shear moduli of the single components, and the lower bounds when these quantities are the corresponding minimum moduli, i.e., we have the upper bound if 1 is the stiffer medium and the lower bound is obtained if 1 is the softer medium (Mavko et al. 2009).

The averages of these bounds are

$$K_s = \frac{1}{2}(K_{\mathrm{HS}}^{+} + K_{\mathrm{HS}}^{-}), \quad \mu_s = \frac{1}{2}(\mu_{\mathrm{HS}}^{+} + \mu_{\mathrm{HS}}^{-}). \tag{4}$$

We also need the dry-rock moduli, K_m and μ_m, and the permeability κ of the layers. Krief et al. (1990) have introduced a model (hereafter called Krief's model) which is consistent with the concept of critical porosity, since the moduli should vanish above a certain value of the porosity (usually from 0.4 to 0.5). Carcione et al. (2000) confirmed that Krief's empirical model is successful at describing the dry-rock moduli of consolidated sandstones. We have

$$K_m = K_s(1-\phi)^{A/(1-\phi)}, \quad \mu_m = \mu_s(1-\phi)^{A/(1-\phi)}, \tag{5}$$

where $A = 3$ hereafter.

Permeability is related to porosity by the Kozeny-Carman relation

$$\kappa_i = \frac{\kappa_{0i}\phi^3}{(1-\phi)^2} \tag{6}$$

(e.g., Mavko et al. 2009), where κ_0 is a reference value. The average permeability is

$$\kappa = \frac{\kappa_1 \kappa_2}{\kappa_1 + \kappa_2}. \tag{7}$$

In this model, the slow mode is due to the different solids and fluid in each layer. If the two solids in each layer are the same, the problem reduces to White's model (White et al. 1975).

2.2 Model 2

This model is based on the composite theory developed by Carcione et al. (2000, 2003, 2005) and Santos et al. (2004), which is summarized in "Appendix 2". Let us omit again the index j for clarity. The (low-frequency) Gassmann bulk modulus of each layer made of a composite medium is

$$K_G = K_m + \alpha^2 M, \quad \alpha = \alpha_1 + \alpha_2, \quad K_m = K_{m1} + K_{m2}, \tag{8}$$

where M and α_i are given in Eq. (24). Moreover,

$$E_m = E_{m1} + E_{m2}, \quad E_{mi} = K_{mi} + 4\mu_{mi}/3, \quad \mu_m = \mu_{m1} + \mu_{m2}, \tag{9}$$

and the permeability of each layer is given by Eq. (7). A suitable generalization for this model to obtain the dry-rock (Krief) moduli is

$$\begin{aligned} K_{mi} &= (K_s/u)\beta_i K_i (1-\phi)^{A/(1-\phi)}, \\ \mu_{mi} &= (\mu_s/v)\beta_i \mu_i (1-\phi)^{A/(1-\phi)}, \quad i = 1, 2, \end{aligned} \tag{10}$$

where K_s and μ_s are the above HS averages, and $u = \sum_i^2 \beta_i K_i$ and $v = \sum_i^2 \beta_i \mu_i$ are Voigt averages (see Carcione et al. 2005).

Then, we apply White's model (17) to obtain the plane-wave modulus. As with Model 1, the slow mode (flow at the interface) is due to the different solids and fluids in each layer.

2.3 Model 3

The third approach considers two cases, where closed and open boundary conditions are assumed at the interfaces and the solids are unmixed (see Fig. 1). A period is composed of four sublayers, where the fractions are

$$p_{ij} = \frac{\phi_{ij} d_j}{(1-\phi_j)\sum_j d_j}, \qquad \sum_i \sum_j p_{ij} = 1, \tag{11}$$

where i and j refer to the sublayer and layer, respectively. As above, the approach requires the dry-rock moduli of each sublayer, given by Krief's model,

$$K_{mi} = K_i(1-\phi)^{A/(1-\phi)}, \qquad \mu_{mi} = \mu_i(1-\phi)^{A/(1-\phi)}, \quad i = 1,2. \tag{12}$$

The permeability of each sublayer is given by Eq. (6).

We consider two sub-models.

Model 3.1 (closed boundary conditions) In this case, there is no flow between the sublayers. For a layered system, Backus averaging applies and the effective modulus along the vertical direction is the Reuss average

$$E = \left(\sum_i \sum_j \frac{p_{ij}}{E_G(ij)} \right)^{-1}, \tag{13}$$

where $E_G = K_G + 4K_m/3$ is the P-wave modulus of each sublayer (Carcione 2014; Eq. 4.11). In this case there is no attenuation and the P-wave modulus does not depend on frequency.

Model 3.2 (open boundary conditions) The solution, if flow is assumed between all the layers, was obtained, implicitly, by Norris (1993) for n layers in a period and by Cavallini et al. (2017) for three dissimilar layers per period. The case of four layers requires to develop the theory explicitly as in the last work. Since this case involves a lengthy development, it is left as future research. To illustrate the differences between models, we consider an example, where two sublayers have the same properties, i.e., a period consist of three layers. The solution is given by Eq. (61) in Cavallini et al. (2017) ($E = p_{33}$) after solving a lineal system (Eq. 64).

To characterize the anelasticity of the P wave normal to layering, we consider

$$\gamma = \mathrm{Re}(E), \tag{14}$$

as the measure of dispersion, and the quality factor

$$Q = \frac{\mathrm{Re}(E)}{\mathrm{Im}(E)} \tag{15}$$

or the dissipiation factor $1000/Q$, to quantify the attenuation (e.g., Carcione 2014).

3 Examples

Table 1 gives the properties of the layers and we consider three values of the hydraulic permeability of the interface: $\bar{\kappa} = 0$ (closed pores), ∞ (open pores) and 10^{-14} m^2 s/kg (mixed or partially open pores). Figure 2 shows the results of Models 1 and 2, which have the same dissipation factor in practice, with relaxation peaks at seismic frequencies and slightly different P-wave moduli, but in practical (experimental) terms these moduli are similar. Decreasing the interface permeability moves the peak to lower frequencies and when the value is zero (closed case) there is no anelasticity, with the predicted modulus equal to the Reuss average of the Gassmann moduli of the single layers, which is also the high-frequency limit of the White model. Note that the amount of dispersion of the open and mixed cases are the same, as shown in Fig. 3 for several values of $\bar{\kappa}$. However, since the attenuation factor is $A \approx \pi f/(cQ)$ (Carcione 2014, Eq. 2.123), where f is the frequency and c is the wave velocity, we have $A_1/A_2 \approx f_1/f_2$. If $f_1 \ll f_2$,

Table 1 Material properties.

Medium	K (GPa)	μ (GPa)	d (cm)	ϕ	η (cP)	κ_0 (darcy)
Layer 1			10			
Solid 1	40	38		0.5	–	10
Solid 2	8	4		0.2	–	10
Fluid	2.25	0		0.3	1	–
Layer 2			5			
Solid 1	40	35		0.6	–	5
Solid 2	30	20		0.3	–	5
Fluid	0.5	0		0.1	100	–

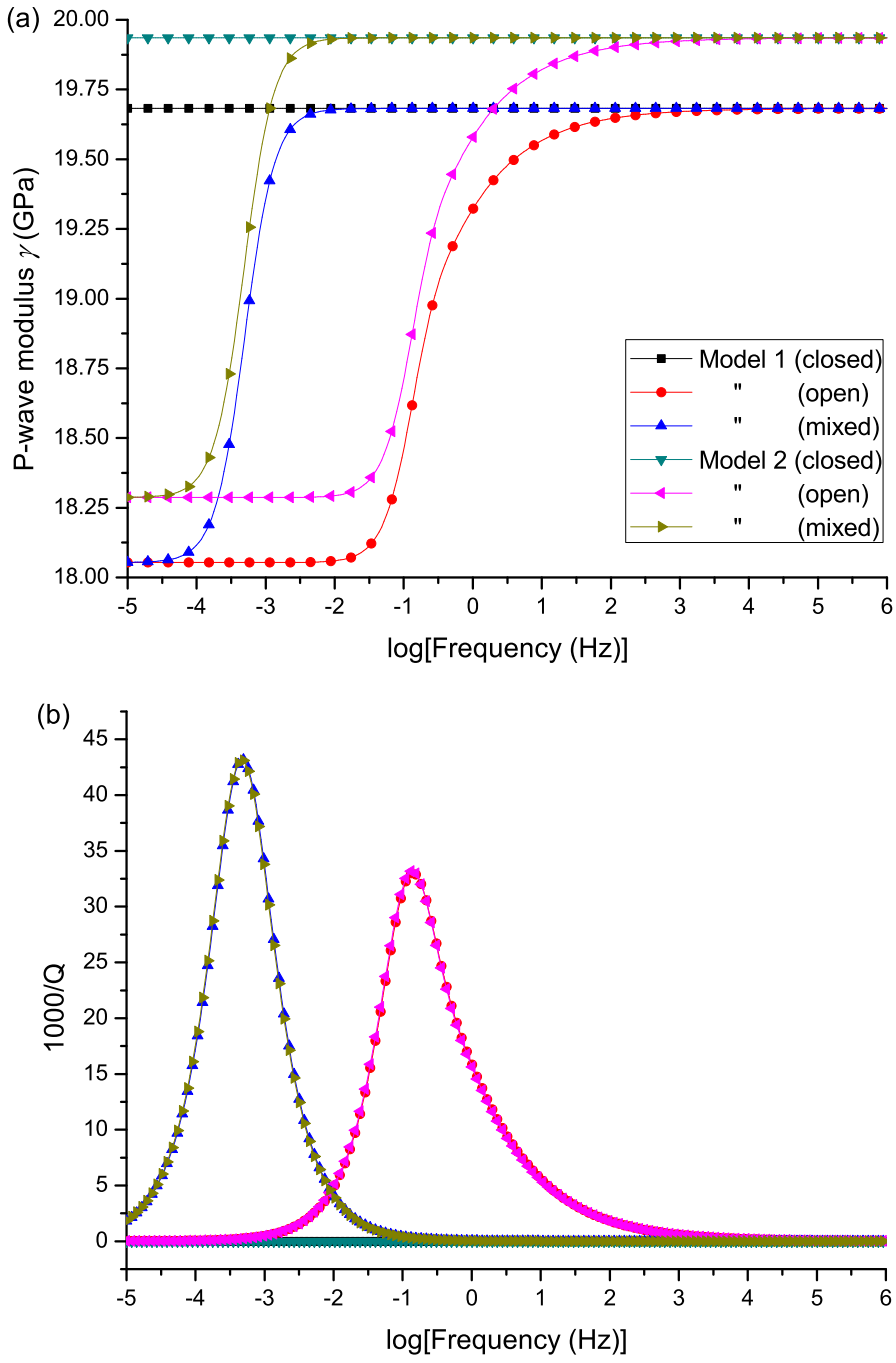

Fig. 2 Dispersion coefficient and dissipation factor, corresponding to Models 1 and 2 for different values of the interface hydraulic permeability [$\bar{\kappa}$ = 0 (closed pores), ∞ (open pores) and 10^{-14} m^2 s/kg (mixed)]. The properties of the media are listed in Table 1 (A= 3). The peaks at low frequencies correspond to the mixed boundary condition

$A_1 \ll A_2$. Figure 2 somehow validates both models, since from a practical viewpoint the results are similar, mainly the attenuation, with the difference that Model 2 is a generalization of the Biot theory to the case of two frames from first principles and predicts additional waves. Therefore, in more general cases, where there is no analytical solution, the two models may differ, with Model 2 predicting more realistic results due to mesoscopic losses (WIFF attenuation),

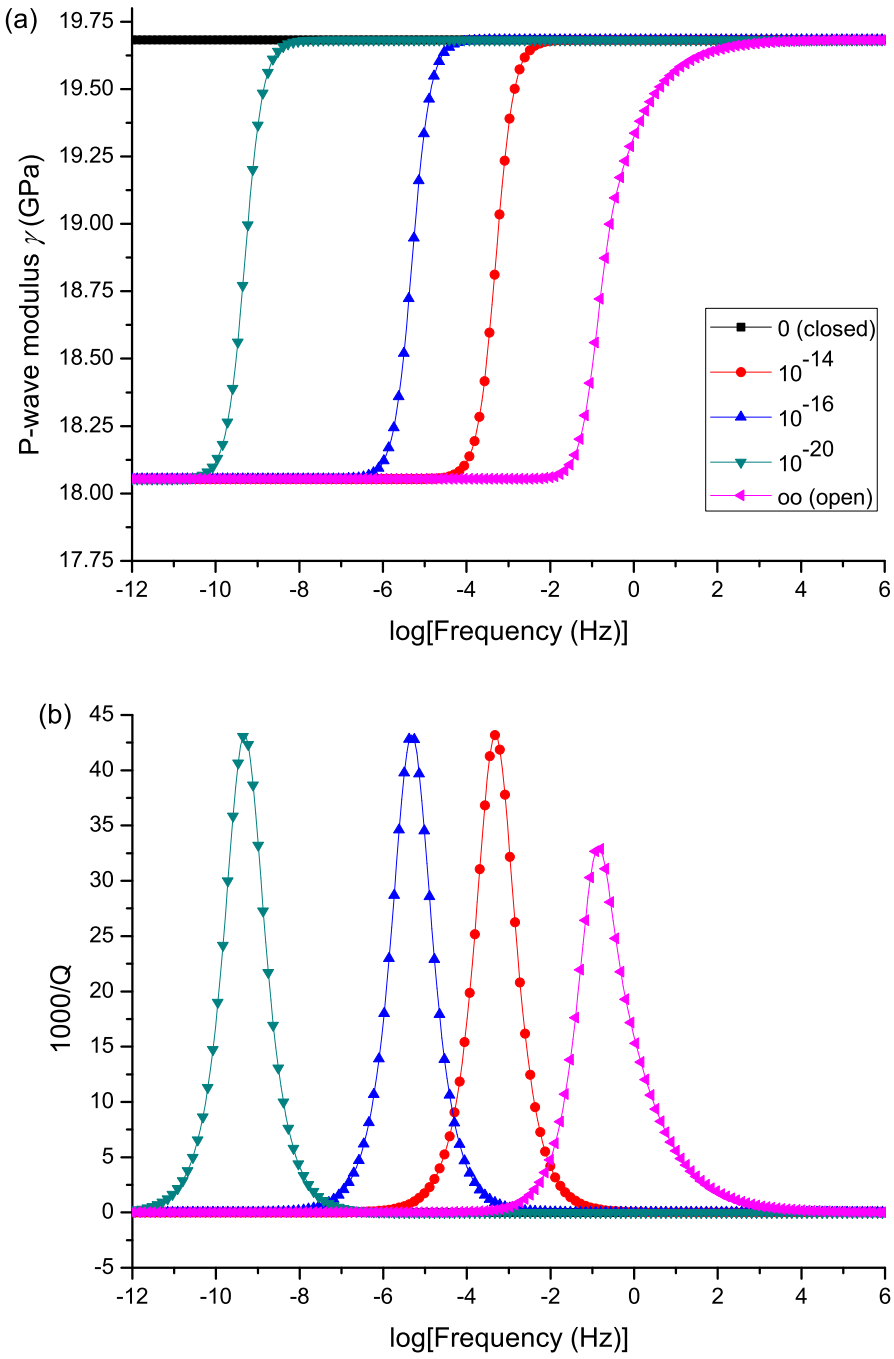

Fig. 3 Dispersion coefficient and dissipation factor, corresponding to Model 1 for different values of the interface hydraulic permeability (units are m^2 s/kg). The properties of the media are listed listed in Table 1 (A= 3)

for instance an extension of the White model to the case of two minerals (or frames).

Let us now consider open boundary conditions at the interfaces and that solid 21 is the same as solid 11 (see Fig. 1). Then, there are three sublayers in Model 3 and we can apply the theory developed by Cavallini et al. (2017) (Model 3.2). Figure 4 compares the results of Models 1 and 2 with those of Model 3. In this case, Models 1 and 2 (black and red symbols) yield a similar result. Model 3.2 predicts the same amount of

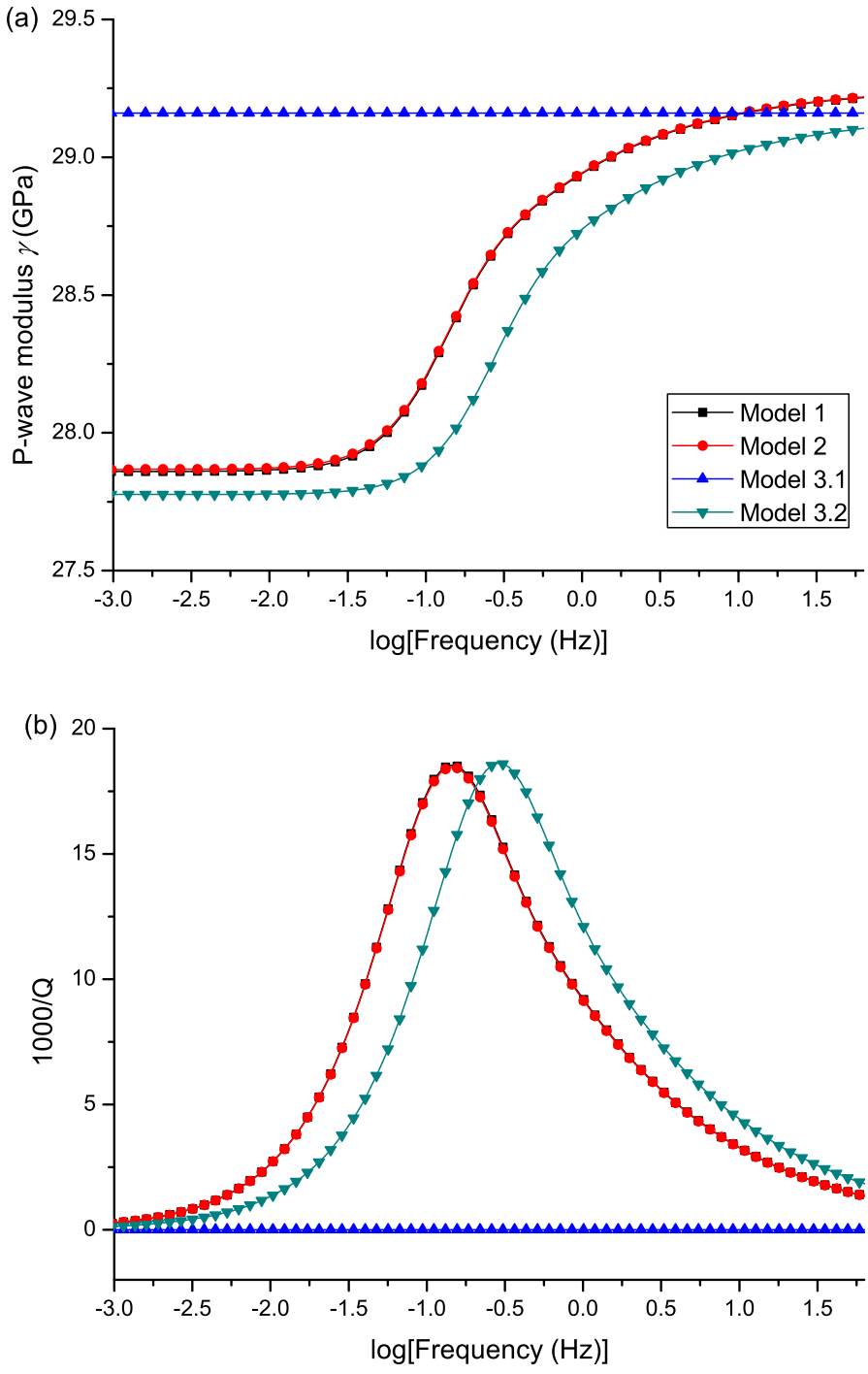

Fig. 4 Comparison of the dispersion coefficient and dissipation factor for the three models. The boundary condition at the interfaces of Models 1, 2 and 3.2 is open and that of Model 3.1 is closed. The properties of the media are listed in Table 1, but solid 21 has been replaced with solid 11 (A= 3). The results of Models 1 and 2 are almost identical

anelasticity and the location of the relaxation peak in the same frequency band, compared to the first two models (0.28 versus 0.14 Hz), despite the fact that the solid phases are segregated, unlike in Models 1 and 2, where the frames are mixed. As expected, Model 3.1 shows no anelasticity. The fact that the first two models yield very similar results is because they are consistent with the Hashin-Shtrikman equations.

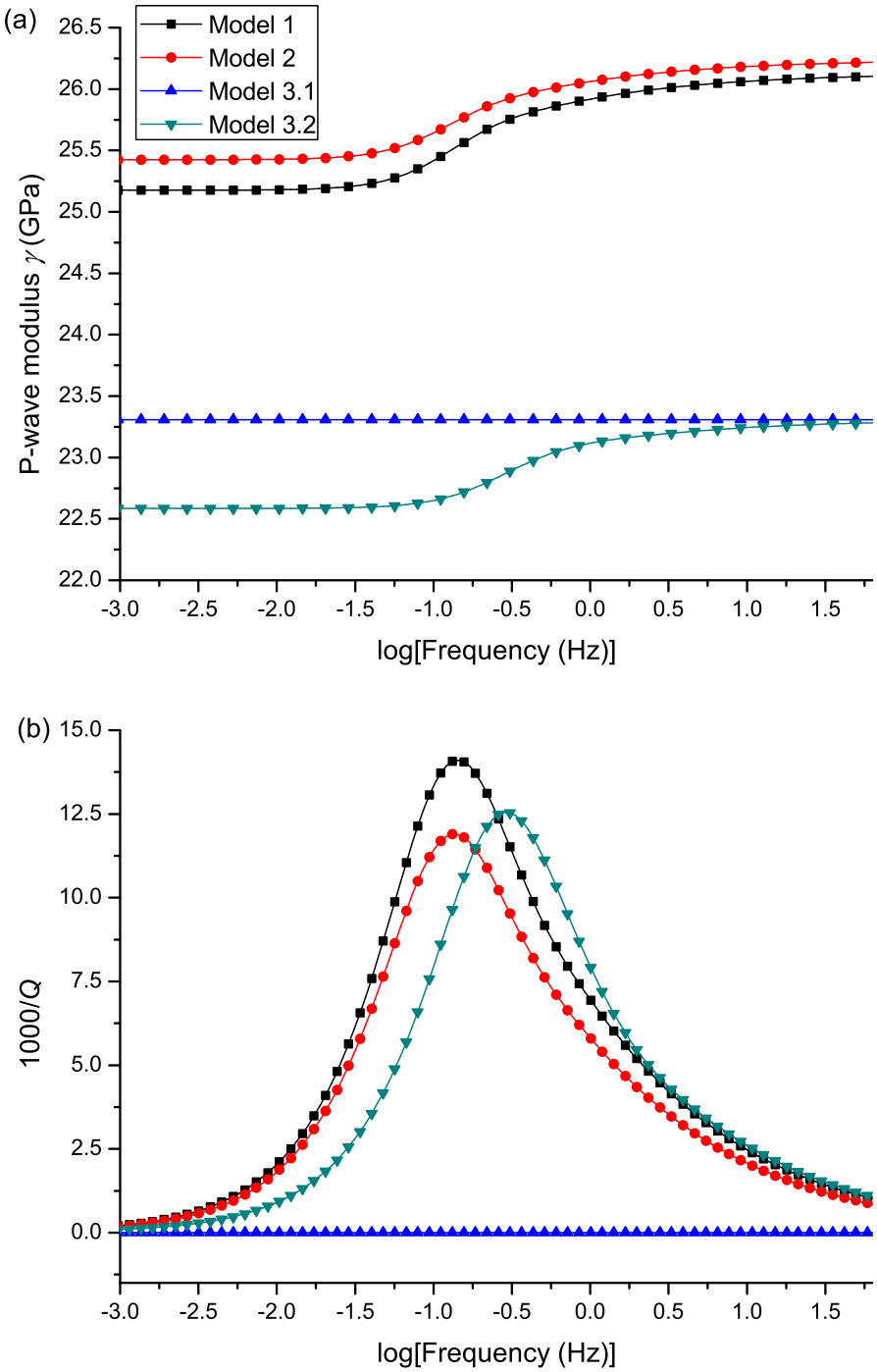

Fig. 5 Same as Fig. 3, but solid 22 has been replaced with solid 21 (see Table 1)

Next, we consider the same comparison of Fig. 4 but replacing solid 22 with solid 21 (see Table 1), keeping the same proportion ($\phi_{22} = 0.3$). In this case (see Fig. 5), Models 1 and 2 predict the same peak location but different peak values of the dissipation factor and slightly different P-wave moduli, although from an experimental point of view these differences are difficult to measure. On the other hand, Model 3.2

Table 2 Material properties.

Medium	K (GPa)	μ (GPa)	d (cm)	ϕ	η (cP)	κ_0 (darcy)
Layer 1			10			
Solid	33	30		0.7	–	10
Fluid	2.2	0		0.3	1	–
Layer 2			5			
Solid 1	33	30		0.35	–	5
Fluid 1	0.5	0		0.15	400	–
Solid 2	10	6		0.35	–	5
Fluid 2	0.0096	0		0.15	0.15	–

predicts a peak of similar strength in the same frequency band.

However, Model 3.2 is essentially different from the first two, not only because the frames are segregated, but because the fluids are also distributed at the mesoscopic scale. In this sense, the White model for thin layers has mesoscopic loss due to these two factors. Let us consider the proportions and properties listed in Table 2, where in Layer 2 there is a different fluid for each sublayer (oil and gas), with different mineral properties as well. In order to use Models 1 and 2, we consider that the effective fluid properties in Layer 2 are given by the Reuss and arithmetic averages, for the modulus and viscosity, i.e.,

$$K_{f2} = \frac{K_{f12}K_{f22}}{K_{f12} + K_{f22}}, \qquad \eta_2 = \frac{1}{2}(\eta_{12} + \eta_{22}). \tag{16}$$

Figure 6 shows the comparison. While the results of Models 1 and 2 coincide and show a single peak, Model 3.2 predicts two relaxation peaks and a lower P-wave modulus. As mentioned above the reason is the different spatial distribution of the solid and fluid phases. In particular, the attenuation in Model 3.2 is higher because of the wave-induced fluid diffusion between fluids 1 and 2 (oil and gas), an effect absent in Models 1 and 2, since the mixing with the Reuss (harmonic) average excludes the presence of the slow diffusive mode. Unlike the classical White model, the results of Model 3.2 show two relaxation peaks (see the explanation in Cavallini et al. 2017).

4 Conclusions

Rocks are composed of many minerals, which affect the seismic properties of thin layering, which here are quantified as modulus dispersion and quality factor. Three different models are considered to obtain the properties perpendicular to layering. They are based on (1) effective properties, (2) Biot-type theory with two mixed frames, and (3) Biot layers with segregated frames. All the models use the White mesoscopic model. The first two models, together with an extension of the White model to the case of partially closed pores at the interfaces, indicate that the location of the relaxation peaks is highly dependent on the interface permeability. Decreasing this quantity moves the peaks to lower frequencies, till the medium becomes lossless for closed pores (no flow).

The general results indicate that Models 1 and 2 predict the same properties in practice, i.e., if subject to experimental measurements. On the other hand, Model 3 with close pores predicts no attenuation, while with open pores the strength and location of the relaxation peak differ from those of the first two models, due to the fact that the frames (and the fluids if there is partial saturation) are segregated at the mesoscopic scale. This study clarifies some aspects of the effects of mineral composition on the seismic properties, namely dispersion and attenuation and provides solutions to test numerical codes, but unfortunately there are no laboratory experiments or field data that consider the analyzed geometry and rheology to compare. A more rigorous analytical solution is to extend the White model to the case of two mineral (or two frames), a task that will be achieved in a future paper, as well the extension to the anisotropic

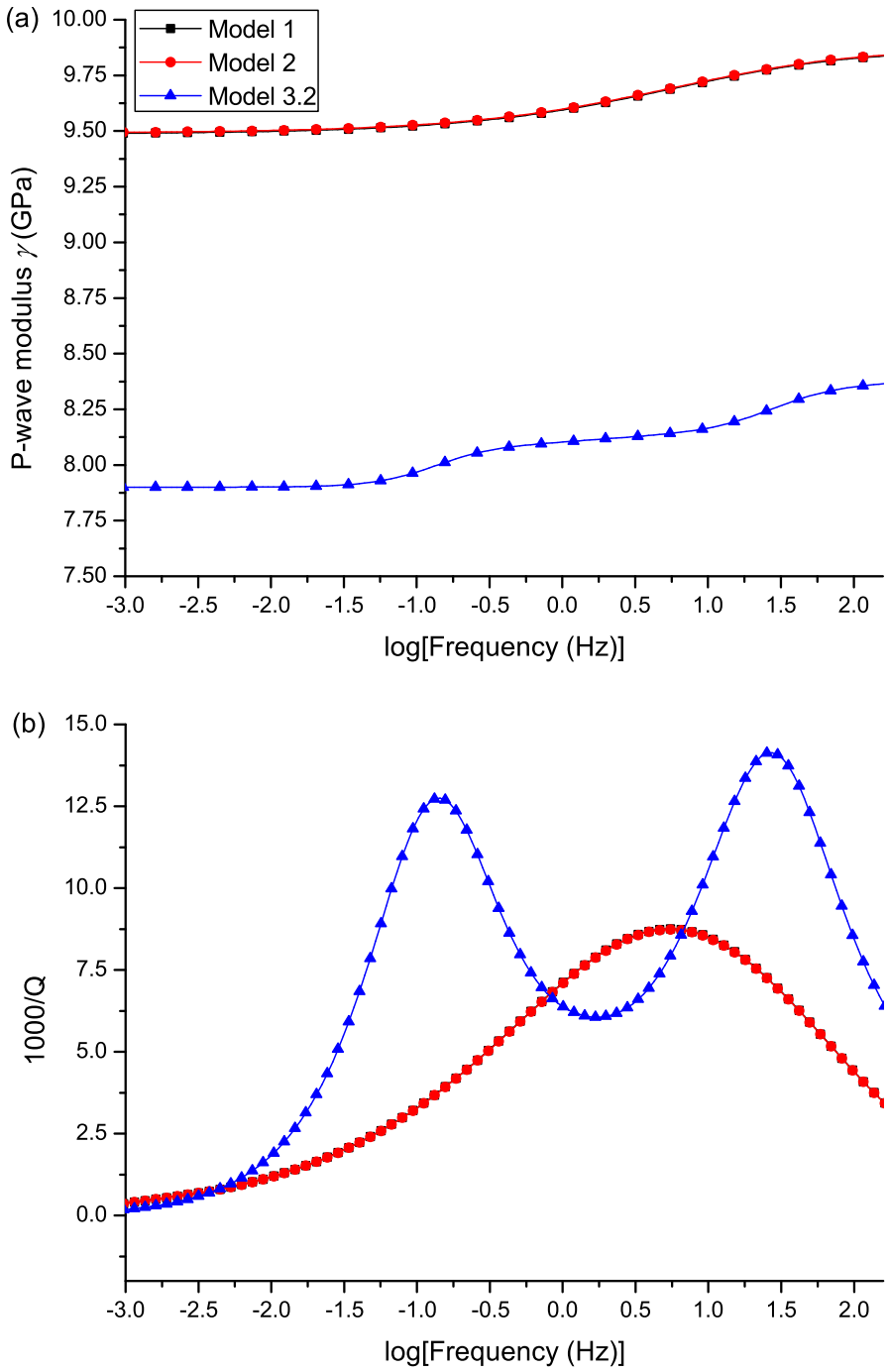

Fig. 6 Comparison of the dispersion coefficient and dissipation factor for the properties given in Table 2. Models 1 and 2 are based on mixed frames, whereas in Model 3.2 the frames are segregated

(transversely isotropic) case, based on the relaxed and unrelaxed elasticity constants.

Acknowledgement The authors are grateful to the support of the National Natural Science Foundation of China (grant no. 41974123), the Jiangsu Innovation and Entrepreneurship Plan, China, and the Jiangsu Natural Science Fund for Distinguished Young Scholars, China.

Appendix 1: White's plane-layer theory with partially-open pore boundary conditions

The model is a stack of two thin alternating porous layers of thickness d_1 and d_2, such that the period of the stratification is $D = d_1 + d_2$ and the proportions of media 1 and 2 are $p_1 = d_1/D$ and $p_2 = 1 - p_1 = d_2/D$, respectively. Each layer is a porous medium composed of one solid and one fluid. The complex and frequency dependent P-wave stiffness for partially open boundary conditions is

$$E = \left[\frac{1}{E_G} + \frac{2(r_2 - r_1)^2}{\mathrm{i}\omega D(I_1 + I_2 + 1/\bar{\kappa})}\right]^{-1}, \tag{17}$$

where $\bar{\kappa}$ is the hydraulic permeability (per unit length) of the interface [see Eq. (19) below for a demonstration], ω is the angular frequency, and omitting the layer subindex j for clarity,

$$r = \frac{\alpha M}{E_G}, \quad I = \frac{\eta}{\kappa a}\coth\left(\frac{ad}{2}\right), \quad a^2 = \frac{\mathrm{i}\omega\eta}{\kappa K_E}, \quad K_E = \frac{ME_m}{E_G}, \tag{18}$$

for each single layer (White et al. 1975; Carcione and Picotti 2006) [see also Carcione (2014, Eq. 7.453)], where κ is the permeability, η is the fluid viscosity, $E_G = (p_1/E_{G1} + p_2/E_{G2})^{-1}$, $E_{Gj} = K_{Gj} + (4/3)\mu_{mj}$ and $E_{mj} = K_{mj} + (4/3)\mu_{mj}$, $M_j^{-1} = (\alpha_j - \phi_j)/K_{sj} + \phi_j/K_{fj}$, $\alpha_j = 1 - K_{mj}/K_{sj}$, $K_{Gj} = K_{mj} + \alpha_j^2 M_j$, with j = 1 and 2 being the two single layers, respectively. Modulus E_G is obtained at high frequencies or $\bar{\kappa} \to 0$. If $\bar{\kappa} \to \infty$, we have the case of open-pore boundary conditions, i.e., complete flow across the interfaces, which is the case of the classical White model.

Equation (17) is based on the boundary condition

$$p_{f1} - p_{f2} = \frac{1}{\bar{\kappa}}\dot{w}_3 \tag{19}$$

Carcione 2014; Eq. 7.404, where p_{f1} and p_{f2} are the fluid pressures in layers 1 and 2, respectively, and w_3 is the relative vertical displacement of the fluid with respect to the solid, which is continuous (the dot above a variable denotes time differentiation). It is straightforward to show that the discontinuity (19) in the fluid pressure at the interface leads to Eq. (17), based on Eqs. 7.443–7.447 in Section 7.13 of Carcione (2014).

The meaning of $\bar{\kappa}$ is explained in Deresiewicz and Skalak (1963) as partially communicating pores between the two media, but can also be related to a thin layer at the interface characterized by the permeability $\bar{\kappa}$. An example is a mud cake much thinner than the wavelength in a borehole (Rosenbaum 1974). A similar Eq. (17) was obtained by Qi et al. (2014), where $1/\bar{\kappa}$ is interpreted as an additional interface impedance due to capillary forces, i.e., exclusively related to the fluids. However, the effect of capillary forces must be considered in the whole pore space to obtain realistic results, as in Santos et al. (2019). Biot's theory does not hold when the rock is saturated by two-phase fluids, since capillary pressure effects and interaction between flows are ignored. Capillary pressure is responsible for the existence of the additional slow wave, where the relative motions between the two fluid phases induce additional energy losses not present in the case of single-phase fluids. These effects induce changes in phase velocities and dissipation factors.

The peak relaxation frequency is approximately given by

$$f_p = \frac{8\kappa K_E}{\pi\eta d^2}, \tag{20}$$

where κ and K_E are obtained harmonic (Reuss) averages, and η as arithmetic average.

The slow P wave is the cause of the attenuation, with a diffusivity constant $D = \kappa ME_m/(\eta E_G)$ (Carcione 2014), and diffusion length $L_r = \sqrt{D/\omega}$. The fluid pressures are equilibrated if L_r is comparable to the layer period. For small L_r for instance (high frequencies), there is not enough time for the pressures to equilibrate, causing anelasticity. Since $\omega = 2\pi f$ and $f = D/(2\pi L_r^2)$, substituting D into this equation, the transition frequency (20) is obtained for a diffusion length $L_r = L_j/4$.

Appendix 2: Constitutive equations for a three-phase composite medium (two solids and one fluid)

The stress–strain relation has been derived by Carcione et al. (2005). We have

$$\sigma_{kl}^{(1)} = [(K_{G1} - \phi\alpha_1\beta_1 M)\theta_1 + M(\alpha_1 - \phi\beta_1)(\alpha_2\theta_2 - \zeta)] + 2\bar{\mu}_1 d_{kl}^{(1)} + \mu_{12} d_{kl}^{(2)},$$

$$\sigma_{kl}^{(2)} = [(K_{G2} - \phi\alpha_2\beta_2 M)\theta_2 + M(\alpha_2 - \phi\beta_2)(\alpha_1\theta_1 - \zeta)] + 2\bar{\mu}_2 d_{kl}^{(2)} + \mu_{12} d_{kl}^{(1)},$$

$$p_f = M(\zeta - \alpha_1\theta_1 - \alpha_2\theta_2), \tag{21}$$

where σ denotes stress components, p_f is the fluid pressure, θ denotes dilatations, $\zeta = -\phi(\theta_f - \beta_1\theta_1 - \beta_2\theta_2)$ is the variation of fluid content, d_{kl} are the components of the deviatoric strain tensor and ϕ is the porosity.

Particularly, the relative displacement of the fluid relative to the solids is

$$w_k = \phi_w[u_k^{(f)} - (\beta_1 u_k^{(1)} + \beta_2 u_k^{(2)})], \tag{22}$$

where u denotes displacements, such that $\zeta = -\text{div } \mathbf{w}$, and the strain components are

$$2\epsilon_{kl}^{(i)} = u_{k,l}^{(i)} + u_{l,k}^{(i)}, \qquad d_{kl}^{(i)} = \epsilon_{kl}^{(i)} - \frac{1}{3}\delta_{kl}\theta_i, \qquad \epsilon_{kk}^{(i)} = \theta_i. \tag{23}$$

The material properties are

$$K_{G1} = K_{m1} + \alpha_1^2 M, \quad K_{G2} = K_{m2} + \alpha_2^2 M,$$

$$M = \left(\frac{\alpha_1 - \beta_1\phi}{K_1} + \frac{\alpha_2 - \beta_2\phi}{K_2} + \frac{\phi}{K_f}\right)^{-1},$$

$$\bar{\mu}_1 = [(1 - g_1)\phi_1]^2\bar{\mu} + \mu_{m1}, \quad g_1 = \mu_{m1}/(\phi_1\mu_1),$$

$$\bar{\mu}_2 = [(1 - g_2)\phi_2]^2\bar{\mu} + \mu_{m2}, \quad g_2 = \mu_{m2}/(\phi_2\mu_2),$$

$$\mu_{12} = (1 - g_1)(1 - g_2)\phi_1\phi_2\bar{\mu},$$

$$\bar{\mu} = [(1 - g_1)\phi_1/\mu_1 + \phi/(\mathrm{i}\omega\eta) + (1 - g_2)\phi_2/\mu_2]^{-1},$$

$$\alpha_i = \beta_i - \frac{K_{mi}}{K_i}, \quad \beta_i = \frac{\phi_i}{1 - \phi}, \quad \beta_1 + \beta_2 = 1, \tag{24}$$

where K_f is the fluid modulus and η is the fluid viscosity; β_i is the fraction of solid i per unit volume of total solid, and g_i are consolidation coefficients of the frames.

The total stress is

$$\sigma_{kl} = \sigma_{kl}^{(1)} + \sigma_{kl}^{(2)} - \phi p_f\delta_{kl} = [(K_{G1} + \alpha_1\alpha_2 M)\theta_1 + (K_{G2} + \alpha_1\alpha_2 M)\theta_2 - M(\alpha_1 + \alpha_2)\zeta]\delta_{kl} + (2\bar{\mu}_1 + \mu_{12})d_{kl}^{(1)} + (2\bar{\mu}_2 + \mu_{12})d_{kl}^{(2)}, \tag{25}$$

where δ_{kl} is Kronecker's delta.

The theory predicts two additional slow P waves and a slow S wave. More details can be found in Carcione et al. (2003).

References

Ba J, Zhao J, Carcione JM, Huang X (2016) Compressional wave dispersion due to rock matrix stiffening by clay squirt flow. Geophys Res Lett 43(12):6186–6195

Ba J, Xu WH, Fu LY, Carcione JM, Zhang L (2017) Rock anelasticity due to patchy saturation and fabric heterogeneity: a double double-porosity model of wave propagation. J Geophys Res Solid Earth 122(3):1949–1976

Backus GE (1962) Long-wave elastic anisotropy produced by horizontal layering. J Geophys Res 67:4427–4440

Brown RJS, Korringa J (1975) On the dependence of the elastic properties of a porous rock on the compressibility of the pore fluid. Geophysics 40:608–616

Carcione JM (2014) Wave Fields in Real Media: theory and numerical simulation of wave propagation in anisotropic, anelastic, porous and electromagnetic media, 3rd edn. Elsevier, Amsterdam

Carcione JM, Picotti S (2006) P-wave seismic attenuation by slow-wave diffusion: effects of inhomogeneous rock properties. Geophysics 71(3):O1–O8

Carcione JM, Gurevich B, Cavallini F (2000) A generalized Biot–Gassmann model for the acoustic properties of shaley sandstones. Geophys Prosp 48:539–557

Carcione JM, Santos JE, Ravazzoli CL, Helle HB (2003) Wave simulation in partially frozen porous media with fractal freezing conditions. J Appl Phys 94:7839–7847

Carcione JM, Helle HB, Santos JE, Ravazzoli CL (2005) A constitutive equations and generalized Gassmann modulus for multi-mineral porous media. Geophysics 70:N17–N26

Carcione JM, Picotti S, Gei D, Rossi G (2006) Physics and seismic modeling for monitoring CO2 storage. Pure Appl Geophys 163(1):175–207

Carcione JM, Morency C, Santos JE (2010) Computational poroelasticity — a review. Geophysics 75(5):75A229–75A243

Cavallini F, Carcione JM, Vidal de Ventós D, Engell-Sørensen L (2017) Low frequency dispersion and attenuation in

anisotropic partially saturated rocks. Geophys J Int 209(3):1572–1584

Carcione JM, Poletto F, Farina B, Bellezza C (2018) 3D seismic modeling in geothermal reservoirs with a distribution of steam patch sizes, permeabilities and saturations, including ductility of the rock frame. Phys Earth Planet Inter 279:67–78

Deer WA, Howie RA, Zussman J (2013) An introduction to rock forming minerals, 3rd edition. The Mineralogical Society

Deresiewicz H, Skalak R (1963) On uniqueness in dynamic poroelasticity. Bull Seism Soc Am 53:783–788

Gei D, Carcione JM (2003) Acoustic properties of sediments saturated with gas hydrate, free gas and water. Geophys Prosp 51:141–157

Hashin Z, Shtrikman S (1963) A variational approach to the theory of the elastic behaviour of multiphase materials. J Mech Phys Solids 11:127–140

Krief M, Garat J, Stellingwerff J, Ventre J (1990) A petrophysical interpretation using the velocities of P and S waves (full-waveform sonic). Log Anal 31:355–369

Mavko G, Mukerji T, Dvorkin J (2009) The rock physics handbook. Cambridge Univ, Press

Müller TM, Gurevich B, Lebedev M (2010) Seismic wave attenuation and dispersion resulting from wave-induced flow in porous rocks: a review. Geophysics 75:75A147-75A164

Norris AN (1993) Low-frequency dispersion and attenuation in partially saturated rocks. J Acoust Soc Am 94:359–370

Pride SR, Harris JM, Johnson DL, Mateeva A, Nihel KT, Nowack RL, Rector JW, Spetzler H, Wu R, Yamomoto T, Berryman JG, Fehler M (2003) Permeability dependence of seismic amplitudes. Lead Edge 22(6):518–525

Qi Q, Müller TM, Gurevich B, Lopes S, Lebedev M, Caspari E (2014) Quantifying the effect of capillarity on attenuation and dispersion in patchy-saturated rocks. Geophysics 79(5):WB35–WB50

Rosenbaum JH (1974) Synthetic microseismograms: logging in porous formations. Geophysics 39:14–32

Santos JE, Ravazzoli CL, Carcione JM (2004) A model for wave propagation in a composite solid matrix saturated by a single-phase fluid. J Acoust Soc Am 115(6):2749–2760

Santos JE, Savioli GB, Carcione JM, Ba J (2019) Effect of capillarity and relative permeability on Q anisotropy of hydrocarbon source rocks. Geophys J Int 218:1199–1209

White JE, Mikhaylova NG, Lyakhovitskiy FM (1975) Low-frequency seismic waves in fluid saturated layered rocks, Izvestija Academy of Sciences USSR. Phys Solid Earth 11:654–659

Zimmerman (1991) Compressibility of sandstones, Developments in Petroleum Science, vol 29. Elsevier, Amsterdam